Bioactive superparamagnetic nanoparticles for multifunctional composite bone cements

Elsevier Editorial System(tm) for Ceramics International

Manuscript Draft

Manuscript Number: CERI-D-19-00671R1

Title: Bioactive superparamagnetic nanoparticles for multifunctional composite bone cements

Article Type: Full length article

Keywords: Superparamagnetic nanoparticles; bioactive nanoparticles; composite bone cement; tumor treatment.

Corresponding Author: Dr. Marta Miola, Ph.D

Corresponding Author's Institution: Politecnico di Torino

First Author: Marta Miola, Ph.D

Order of Authors: Marta Miola, Ph.D; Anuj Bellare; Francesco Laviano; Roberto Gerbaldo; Enrica Vernè

Abstract: Magnetite-based nanoparticles (NPs) were synthesized by co-precipitation process and coated with a thin layer of silica, eventually doped with calcium, by a modified Stöber method. The potential bioactive behavior of NPs was investigated by dipping samples in simulated body fluid (SBF) and analyzing them with Field-Emission Scanning Electron Microscope (FESEM) equipped with Energy Dispersive Spectroscopy (EDS). Silica-coated NPs displayed evidence of HAp grown on their surface and were then used as a filler for polymethyl methacrylate (PMMA)-based bone cement to impart bioactive and magnetic properties. The influence of the amount of magnetic NPs and the cement mixing method (manual or mechanical) were estimated in terms of NPs dispersion, compressive strength and bioactive behavior. The obtained data evidenced that both the NPs amount and the mixing method influenced the strength of the composites. A delay in the bioactivity was observed for manual mixed cement; moreover, mechanically mixed composites containing a low amount of NPs showed superparamagnetic behavior. These results suggest that the investigated composite bone cements are promising materials for the treatment of bone tumors and associated complications.

POLITECNICO
DI TORINO
Dipartimento
di Scienza Applicata
e Tecnologia

Turin, January 18, 2019

Dear Editor,

I would like to submit, for a possible publication on the Journal "Ceramics International", the original paper:

"Bioactive superparamagnetic nanoparticles for multifunctional composite bone cements"

Submitted by:

Marta Miola[1], Anuj Bellare[2], Francesco Laviano[1], Roberto Gerbaldo[1], Enrica Verné[1]

1 Institute of Materials Physics and Engineering, Department of Applied Science and Technology, Politecnico di Torino, C.so Duca degli Abruzzi 24, 10129 Torino, Italy

2 Department of Orthopedic Surgery, Brigham & Women's Hospital, Harvard Medical School, 25 Shattuck Street, Boston, MA, 02115

In the authors' opinion this article could improve the knowledge regarding the surface treatment of the superparamagnetic nanoparticles and the coating with silica. Moreover it can contribute to open new insights on the design of innovative PMMA-based bone cements.

Authors confirm that this manuscript is original and has not been previously published in other journals, nor is it submitted to other journals at this present time and we support that do not exist conflict of interest with no academic institution or company. Moreover, authors declare that, if the article will be accepted, it will not be published elsewhere in the same form and in any language, without the written consent of the publisher.

*** Corresponding author:**

Dr. Marta Miola

Politecnico di Torino

Department of Applied Science and Technology (DISAT)

Corso Duca degli Abruzzi 24, 10129 Torino, ITALY

Tel.: +39-0110904717

Fax: +39-0110904624

e-mail: marta.miola@polito.it

Marta Miola
Dipartimento di Scienza Applicata e Tecnologia
Politecnico di Torino Corso Duca degli Abruzzi, 24 – 10129 Torino – Italia
tel: +39 011.090.4717 fax: +39 011.090.4624
marta.miola@polito.it
http://www.composites.polito.it

Response to reviewer

We thank the Editor and the Reviewer for the useful suggestions to further improve the quality of our work. The response to reviewers and all the corrections or integrations performed in the revised manuscript are highlighted in the response to reviewers and in the text in red colour.

Reviewer's comments:

Reviewer #1: This work provides results that may be of interest in biomedical applications , i.e. "a novel approach was used to develop a composite bone cement containing magnetic nanoparticles useful for hyperthermic treatment and at the same time be able to integrate with host tissue". Some extremes have to be taken into account to improve the MS:
1)In the discussion the sentence "the presence of silica coating appears to influence the mechanical strength, because probably it changes the properties at the interface. This reduction was not observed in the composites containing 10 wt% of NPs, in which the compression strength was most likely influenced by the amount of NPs" is not clear, need explanation.

A: The parameters that can influence the mechanical strength of the composite are: i) the method of mixing, ii) the amount of the NPs and the properties at the interface NPs/cement. For composites containing 5% of NPs, authors observed a decrease of strength for samples containing magnetite-silica (MS) NPs; while they noticed a comparable strength for samples containing 10% of magnetite (M) and MS NPs. Moreover the strength values of 10% containing samples are comparable with values obtained with 5% MS-containing composites (both manually and mechanically mixed). Therefore, authors supposed that up to 5% of NPs the presence of silica coating appears to be the key factor that influence the mechanical strength, while introducing 10% of NPs the mechanical strength seems to be more influenced by the amount of NPs rather than by the silica coating. The discussion has been implemented in the manuscript.

2)The number of FESEM-EDX figs. and micrographs can be reduced . Some of them are out of focus (Fig.1b,c)

A: The number of FESEM images in figures 1, 2 and 3 has been reduced as suggested; moreover, the micrograph of magnetite in figure 1 has been substituted.

3) The recent review paper : A.G.Roca,L.Gutiérrez,H.Gavilán,et al.,Design strategies for shape-controlled magnetic iron oxide nanoparticles, Adv. Drug Deliv. Rev., https://doi.org/10.1016/j.addr.2018.12.008 , must be taking into account.

A: Authors would like to acknowledge the reviewer for the kind suggestion; even if the paper does not discuss about the design of the used nanoparticles, but it is focused on the role of silica shell in the bioactivity mechanism of magnetic NPs, the proposed review has been mentioned in the introduction.

Bioactive superparamagnetic nanoparticles for multifunctional composite bone cements

Marta Miola[1*], Anuj Bellare[2], Francesco Laviano[1], Roberto Gerbaldo[1], Enrica Verné[1]

[1] Institute of Materials Physics and Engineering, Department of Applied Science and Technology, Politecnico di Torino, C.so Duca degli Abruzzi 24, 10129 Torino, Italy

[2] Department of Orthopedic Surgery, Brigham & Women's Hospital, Harvard Medical School, 25 Shattuck Street, Boston, MA, 02115

* Corresponding author

Abstract

Magnetite-based nanoparticles (NPs) were synthesized by co-precipitation process and coated with a thin layer of silica, eventually doped with calcium, by a modified Stöber method. The potential bioactive behavior of NPs was investigated by dipping samples in simulated body fluid (SBF) and analyzing them with Field-Emission Scanning Electron Microscope (FESEM) equipped with Energy Dispersive Spectroscopy (EDS). Silica-coated NPs displayed evidence of HAp grown on their surface and were then used as a filler for polymethyl methacrylate (PMMA)-based bone cement to impart bioactive and magnetic properties. The influence of the amount of magnetic NPs and the cement mixing method (manual or mechanical) were estimated in terms of NPs dispersion, compressive strength and bioactive behavior. The obtained data evidenced that both the NPs amount and the mixing method influenced the strength of the composites. A delay in the bioactivity was observed for manual mixed cement; moreover, mechanically mixed composites containing a low amount of NPs showed

superparamagnetic behavior. These results suggest that the investigated composite bone cements are promising materials for the treatment of bone tumors and associated complications.

Keywords

Superparamagnetic nanoparticles, bioactive nanoparticles, composite bone cement, tumor treatment

1. Introduction

The surgical treatment of primary (i.e. osteosarcoma, chondrosarcoma, Ewing sarcoma) and secondary (metastases) malignant bone tumors, consists in the removal of the tumor mass followed by wide-excision of the surrounding tissue. Patients often undergo an amputation and prosthesis application. Benign tumors (osteoma, osteoblastoma, osteochondroma) usually need less bone tissue curettage but have a high relapse frequency: thus, even in these cases, prosthesis is one of the most common solutions of reconstruction. Most patients with bone cancer in a limb undergo surgery and, in turn, need reconstructive surgery to maximize limb function [1]. The traditional approaches for these types of tumors, including chemotherapy and radiotherapy associated with surgery, are not always completely satisfactory [2,4] and contemplate the occurrence of an invalidating prosthetic treatment.

During the past, physicians have tried to utilize artificial temperature elevations for the treatment of tumor diseases. Today, this approach uses a variety of temperature ranges (from 39 – 40 °C up to 80 – 90 °C) and, accordingly, a great number of techniques to induce those temperatures under controlled conditions. The European

Society for Hyperthermic Oncology (ESHO) [5] officially recognized the hyperthermia treatment in oncology as "*the therapy which uses the generation of a higher temperature at a tumor-involved region of the body*". It has been widely recognized that the most beneficial contribution of hyperthermia for oncological treatments is based on the enhancement of the effectiveness of other treatments (radiotherapy, chemotherapy, radiochemotherapy, gene therapy, immune therapy, etc.) without additional toxicity. Actually, the prevalent clinical application of this therapy is the hyper thermal perfusion chemotherapy, or the increase of temperature by means of microwave or radiofrequency devices. A major limitation of these procedures is the need to repeat the treatments by means of invasive approaches, if a single treatment is not sufficient [6]. The use of implantable magnetic materials has also been attempted to overcome the limits of hyper thermal perfusion, with a specific indication for bone tumors [7-9]. These materials can be implanted into the cavity created by the removal of the tumor, and can be heated by using an alternating magnetic field, through hysteresis loss and induced eddy currents, causing the indirect heating of nearby tissue. Up to now, the magnetic materials used for this purpose comprise metal alloys (Fe, Co, Ni), oxides (Fe_2O_3, Fe_3O_4), ferrites ($LiFe_5O_8$, $MgFe_2O_4$) [10,11,12], often as nano-sized particles dispersed in different matrices (albumin, polymers, ceramic materials). The principal disadvantages are that, for their use, some of these materials (such as the metal alloys) require the application of a very intense alternating field, difficult to realize in a hospital. In addition, they often have very complex formulations [8] and some of them are not always biocompatible. Furthermore, all these materials are unlikely to integrate with the tissues, since they are based on bio-inert formulations and, due to the unreliable rise in temperature, are not clinically used.

Moreover, they are not able to prevent the primary associated complications such as fractures, delayed union and pseudo-arthrosis [7]. Acrylic cement is frequently used as a bone filler in the case of tumor, but it still has many shortcomings, such as low osteointegration. Several additives are proposed to address these shortcomings [13] like bioactive glasses, glass-ceramics and hydroxyapatite [14] to promote both bone bonding and mechanical properties. On the other hand, bone cements containing magnetic nanoparticles were also explored [15-17]; however, these materials are not osteointegrable. An approach to the development of bone fillers with both magnetic and bioactive properties has been reported by using materials of complex formulations (containing several phases, one for each needed feature) and without a systematic study of the proper frequency and intensity of the electromagnetic filed needed for their activation [18]. In summary, none of these strategies is able to impart to an oncological bone implant all the above mentioned properties by the use of a unique multifunctional material, minimizing the influence of the different additives on its structural and handling properties. In previous papers [19-21] a bioactive and ferrimagnetic glass–ceramic containing magnetite as crystalline phase, has been developed by E. Verné and co-workers, as filler for PMMA based bone cements, with successful results in terms of mechanical properties, bioactivity, biocompatibility, ability to generate heat when activated by an alternating magnetic field, as well as selective tumoral cell death by apotosis under exposure to magnetically induced hyperthermia. In the present paper we advanced the concept of multifunctional stimuli-responsive composite bone cements for the treatment of bone tumors and associated complications, by using silica coated magnetite superparamagnetic nanoparticles as a filler, which displayed for the first time in literature a bioactive

behavior. The development of bioactive and magnetic Fe-Ga nanoparticles were reported by Sanchez et al., [22]; however, in this study a biomimetic method was adopted to induce bioactivity. Instead, the magnetic nanoparticles developed in this work possess an intrinsic bioactive behavior due to the presence of the silica shell and thus of Si-OH groups, which act as sites for apatite nucleation.

2. Experimental

2.1 Synthesis of magnetic nanoparticles

2.1.1 Iron Oxide nanoparticles synthesis (M)

Magnetic nanoparticles (magnetite-based nanoparticles-M) were synthesized using reactants purchased from Sigma-Aldrich© (St Louis, MO, USA) by employing a protocol adapted from literature [23,24]. The co-precipitation method of nanoparticle fabrication was used, by mixing 37.5 ml of 0.1 M ferrous chloride tetrahydrate ($FeCl_2*4H_2O$) solution and 50 ml of 0.1 M ferric chloride hexahydrate $FeCl_3 * 6H_2O$) solution, under mechanical stirring (35 W Overhead mechanical stirrer, single shaft 300 rpm) while monitoring the pH of the solution. Ammonia was added dropwise until a pH of 9.5 – 10 was attained and the solution became black due to co-precipitation of nanoparticles. It is expected that a mixture of magnetite and maghemite should be obtained since the synthesis was performed in air, as previously reported in the literature [25,26]. The solution was then subjected to ultrasound for 20 min and it was subsequently washed in two steps. Firstly, the suspension was separated under a magnetic field using a magnet and the clear solvent was removed using a pipette. This step was repeated three times while adding bi-distilled water to remove unreacted chlorides and ammonia. A solution of citric acid (CA) 0.05 M was used to achieve

good dispersion and prevent further agglomeration [27]. The addition of citric acid to the suspension lowered the pH to about 2.8 – 2.9.; then the pH was increased to 5.2 to increase the adsorption rate. As expected, the citric acid with a pH of 5.2 showed two carboxylic deprotonated groups that interacted with the -OH groups on the nanoparticles. The suspension was then placed in orbital shaker (KS 4000i control, IKA®) maintained at 80 °C and operating at 150 rpm for 90 minutes to allow functionalization of the nanoparticles [24].

In the second washing step, a Millipore ultrafiltration device was used (Solvent Resistant Stirred Cells – Merck Millipore). The nanoparticles suspension was washed twice with twice-distilled water and re-suspended in twice-distilled water, while maintaining the pH at about 11 using ammonia, to maximize the nanoparticles dispersion. In a low basic environment the deprotonation of the third -COOH group of citric acid is expected, enhancing electrostatic repulsion of the nanoparticles and their dispersion in water [24].

2.1.2 Coating of iron oxide nanoparticles with silica shell (MS)

The iron oxide nanoparticles stabilized with CA were then coated with a silica shell following the Stöber method [28]. Tetraethyl orthosilicate (TEOS) was used as silica precursor in a mixture of ethanol and water (ethanol:water ratio was 4:1). Ammonia was added to obtain a pH value of around 10 and the solution was kept in an orbital shaker at 25 °C for 3 hours. Afterwards, a Millipore ultrafiltration device was used to twice wash the suspension and remove unreacted reagents. Coated nanoparticles were then re-suspended in water.

*2.1.3 Coating of iron oxide nanoparticles with calcium-doped silica shell (*MSCa-C, MSCa-H)

For comparative purposes, with respect to the NPs bioactivity, iron oxide nanoparticles stabilized with citric acid were also coated with a calcium doped silica shell because calcium is well known for its role in the bioactivity mechanism of silica based bioactive glasses [29,30]. In fact, glasses in the $CaO–SiO_2$ binary system have been recognized as basic components for the most common bioactive glass compositions. It is reported that calcium ion dissolution from the glass network induces the formation of silanols (Si–OH) on the surface, due to ion exchange with H_3O^+ ions, and increases the degree of supersaturation of the simulated body fluid with respect to hydroxyapatite. Thus, the presence of silanol groups on the surface of a bioactive glass and the release of Ca^{2+} ions are both important issues to induce nucleation of hydroxyapatite on a silica-based bioactive material.

For this purpose, iron oxide nanoparticles with a calcium-doped silica shell were also synthesized, by adapting the sol-gel process used for bioactive glasses, as reported in Borroni et al. [24]. Although calcium nitrate is usually adopted for the synthesis of sol-gel glasses, in the present work it was not used, since it requires high temperature thermal treatment (more than 600 °C) to include calcium ions in the silica network. At these temperatures the structure and properties of magnetite nanoparticles can be altered [31]. Thus, calcium citrate and calcium hydroxide (Sigma Aldrich) were selected as precursors, to prepare calcium doped silica coated magnetite (named MSCa-C and MSCa-H, respectively). Calcium ions were introduced into the iron oxide nanoparticles synthesis solution in the Si:Ca ration of 99:1. Aqueous solutions of calcium citrate (0.85 g/l) and calcium hydroxide (0.015 M) were prepared and added to TEOS, ethanol and

water. The suspension was maintained at 25 °C for 3 h, the obtained nanoparticles were then washed using the ultrafiltration device and re-dispersed in twice-distilled water.

2.2 Morphological and compositional characterization of nanoparticles

The nanoparticles morphology, their size distribution and the presence of silica shell were investigated using FESEM (Field-Emission Scanning Electron Microscope - SUPRATM 40, Zeiss, Germany) equipped with Energy Dispersive Spectroscopy (EDS). TEM investigation of nanoparticles obtained using the same synthesis route have been reported previously [24].

2.3 Bioactivity test on nanoparticles

The bioactivity test was performed in two different ways: in the first experiment, all synthesized nanoparticles (M, MS, MSCa-C, MSCa-H) were dried in an oven at 60°C, subsequently 5 mg of powder was re-dispersed in 50 ml of simulated body fluid (SBF – Kokubo [32]), maintained in an orbital shaker at 37 °C for 2 weeks. At the end of the test, the powders were dried and fixed on adhesive carbon tape on stub supports for the FESEM and EDS analysis.

In the second experiment, only MS and MSCa-H were tested based on the results obtained from the first experiment. In this case, in order to avoid particles agglomeration during the drying process, 100 μl of nanoparticles suspension were mixed with 50 ml of SBF and placed in the orbital shaker at 37 °C for 2 weeks. At the end of the experiment, the SBF was removed, the nanoparticles were gently washed with twice-distilled water and a drop of solution containing the nanoparticles was

deposited on a copper TEM grid with carbon film (SPI Supplies® Brand Lacey Carbon Coated 200 Mesh Copper Grids – JEOL S.p.A.) for FESEM-EDS analyses.

2.4 Synthesis of magnetic NPs/PMMA nanocomposite bone cements

Composite bone cement samples were prepared incorporating only iron oxide (M) and silica-coated iron oxide nanoparticles (MS) on the basis of the results obtained from nanoparticle characterization, particularly from the bioactivity evaluation.

Commercial bone cements, like the Surgical Simplex© P (Stryker Orthopaedics Inc, Mahwah, NJ) used in this work, are provided in two-components in the form of a powder and a liquid, respectively. The two components are mixed directly in the operating room and a free-radical polymerization of the monomer occurs when the initiator contained in the powder is mixed with the accelerator contained in the liquid monomer. The bone cement viscosity changes over time from a slurry into dough like state that can be safely applied and then finally hardens into solid material [33].

The Simplex© bone cement powder consists in 15% (by weight) of PMMA, 75% of MMA-styrene copolymer (named simply *PMMA powder* from now on), 1.5 % BPO (benzoyl peroxide initiator) and 10% barium sulfate as radio-opaque phase. The liquid component consists of 97.4 % MMA, 2.6 % DMPT (N,N-Dimethyl-p-toluidine activator) and 89 ppm of hydroquinone stabilizer. The preparation of the plain bone cements consisted of the following steps:

i. PMMA powder was placed in the mixing cartridge (40 g)
ii. The monomer was added (20 ml).
iii. The slurry was stirred for 1 minute. During mixing, after 20 seconds, total wetting of the powder by the monomer was achieved.

iv. The obtained dough was extruded using a Stryker cement gun into molds to fabricate mechanical test specimens. Hardening was complete after 7 – 9 minutes.

2.4.1 Investigation of the sequence for bone cement synthesis

The nanocomposite bone cement was prepared by following different strategies. Three methods of mixing were investigated in order to determine the best mixing sequence to be followed in the production of the samples. In each case, the amount of nanoparticles was estimated to be 10% by weight relative to the polymeric powder. For these tests only pure magnetite powder was used (Composite samples named S+M).

Method # 1: the magnetic suspension of nanoparticles functionalized with citric acid was dried at 60 °C and dispersed in the liquid MMA in an ultrasound bath for 10 min. Then MMA + NPs and PMMA powder were mixed together.

Method # 2: the magnetic suspension of nanoparticles functionalized with citric acid was mixed with ethanol directly in the PMMA powder. The mixture obtained was dried overnight at 37 °C. Subsequently MMA was added to for the synthesis of cement.

Method # 3: In this method, pure magnetic nanoparticles were separated from the liquid and re-dispersed in MMA by decanting the water after separation of the suspension using a magnet (without drying the particles). The liquid monomer was added to the wet particles and thereafter mixed with PMMA powder. The presence of water, which remains adsorbed on NPs, reduced the duration of the polymerization.

The first mixing sequence (*Method # 1*) appeared to be the most appropriate as determined by preliminary SEM characterization, and was adopted for all the

subsequent preparations. The liquid suspension of magnetic nanoparticles was dehydrated in an oven at 60 °C prior to preparation of composite cements. During the dehydration process, it is possible to lose the nano-metric structure, so the dried powders were fragmented using mortar and pestle and subsequently its suspension in monomer was subjected to 30 minutes of ultrasound to reacquire the initial nanoscale dispersion.

2.4.2 Synthesis of composite bone cements: mixing methods

The mixing step was then further optimized, in order to evaluate the efficacy of hand and mechanical mixing, as follows. Both 10 wt% and 5 wt% of nanoparticles by weight of cement powder was evaluated.

Hand mixing

A normal cartridge mixer was employed, using the following procedure:

i. the powder was placed in the cartridge
ii. the liquid monomer containing the dispersed nanoparticles were added
iii. the cartridge mixer was closed
iv. the vacuum pump was turned on
v. the cement was agitated and mixed by moving up and down the upper ring of the device
vi. the cement was shaken for one minute
vii. the vacuum pump was turned off and the cartridge was inserted into the cement gun

Three kind of materials were prepared: pure Simplex© as already used in clinical applications (S), Simplex© + pure magnetite nanoparticles (S+M) to evaluate the

dispersion of the magnetic material into the acrylic cement and Simplex© + silica coated magnetite nanoparticles (S+MS) as the final nanocomposite. As previously mentioned, Ca-doped MS were not used as filler based on the results obtained from bioactivity test.

Mechanical mixing

For mechanical mixing, the cartridge mixer was modified in order to fix the stirring shaft into a standard chuck. The upper ring was cut and the plastic collar was contoured to fasten it through the jaws without introducing eccentricity in the rotation of the shaft. In this manner, it was possible to control the mixing speed using the overhead mechanical stirrer controls (IKA©, the EUROSTAR power control-visc), like the one used in the nanoparticle preparation. Vacuum mixing was also employed in this method using a vacuum pump. The maximum possible output recorded on the shaft was 105 W with a chuck torque of 60 N·cm and a speed between 50 and 2.000 rpm.

There were two methods employed in the preparation of the nanocomposite samples. One uses the same hand mixing with the mixing cartridge under vacuum; the second uses the overhead mechanical stirrer to perform a high speed agitation. Four different speeds were investigated (250, 500, 1000, 1500 rpm) in order to compare the compressive strength of the cement compared to that of hand mixed cements. Pure Surgical Simplex© P was used for this test. Each trial was conducted following the ISO 5833 standard [34]. During this test, the working time of cements was evaluated, in order to verify any correlation with the mixing speed.

The best two preparation methods were finally used to cast all samples needed for the complete mechanical, morphological and *in vitro* characterizations. All samples were machined for a better grade of finish. Seven groups of cements were prepared:

2.5 Morphological-compositional and physical characterization

Morphological-compositional characterization of the composite bone cements was performed by means of field emission scanning electron microscopy (FESEM, SUPRATM 40, Zeiss) equipped with energy dispersive X-ray spectroscopy (EDS).

Density measurement was carried out on the commercial cements using the *Mohr's balance* in order to estimate eventual differences between manually and mechanically mixed cements.

2.6 Mechanical characterization of nanocomposite bone cements: compression test

Following the ISO standard 5833-2002 [34], compression tests were performed in order to assess the mechanical behavior under compression load. Cements with all concentrations of nanoparticles were investigated and compared with the pure PMMA-based Surgical Simplex© P.

A Single Column Frame eXpert 5601 Modular Universal Testing Systems with the eP2 Digital closed loop servo controller and CPC-116-B-AL platens (Admet Inc, Waltham, MA) was used to determine the compressive strength of the samples. In according with the standard, samples were mixed for 1 min and cast into a stainless steel mold with five cylindrical holes (inner diameter 6 mm, inner depth 12 mm) for 24 hours.

The samples were taken out from the mold after they had fully set and using emery paper to reduce the stress concentration at the edges of the cements. In some cases, the superior and inferior faces were machined with a laser cut edge in order to create two parallel surfaces. The compression test was, then, performed according to Annex E

of the ISO standard [34]. This test was performed on at least 5 specimens for each type of material.

2.7 Bioactivity evaluation of the nanocomposite cements

The study was planned to evaluate different stages of bioactivity of composite samples (Simplex© P + magnetite-silica, 5 and 10%wt) immersed in SBF [31] for different lengths of time (7, 14 and 30 days) in an incubator at 37 °C ± 1,5 °C, as conducted on pure nanoparticles

The solution was refreshed every 2-3 days. During refreshes pH values were recorded in order to monitor if ions release could change the pH of solution appreciably.

The amount of SBF solution (25 ml) was defined in accordance to Kokubo's protocol. When the samples were removed from the SBF they were gently rinsed in twice-distilled water and left to dry at room temperature [32]. Characterization after soaking in SBF was performed by FESEM-EDS analyses.

2.8 Magnetic characterization of composite bone cements

The magnetic properties of composite cements (containing 5 wt% NPs and mechanically mixed) were investigated with a DC magnetometer/ AC susceptometer (Lakeshore 7225) equipped with a Cryogen-Freemagnet at room temperature in quasi static condition.

Magnetic hysteresis cycle measurements were performed using a magnetic field up to 800 kA/m, in order to estimate the main magnetic parameters of the materials and the influence of the silica coating.

3. Results

3.1 Magnetic nanoparticles characterization

All the prepared NPs exhibited a magnetic response (Figure 1a). As reported in a previous study [24] all the synthesized NPs revealed superparamagnetic behavior, with saturation values in a range of 30-60 emu/g and no coercivity. Figure 1a reports the magnetic attraction of the dried magnetite (M) powders.

SEM image (Figure 1b) of M nanoparticles showed evidence of a pseudo spherical shape with diameter between 5 and 15 nm. The EDS compositional analysis (Figure 1c) revealed peaks of iron (Fe) and oxygen (O). All other elements, such as copper (Cu) or carbon (C) that appeared on the spectrum came from the stub and the grid.

The silica-coated magnetite nanoparticles (MS) and Ca-containing magnetic nanoparticles did not revealed any substantial differences in comparison with pure magnetite (M) in terms of size and morphology (data not reported). EDS analysis of MS showed evidence of the presence of a silicon peak (Figure 1d) in addition to iron and oxygen; while EDS analysis of MSC-H (Figure 1e, as example) showed evidence of a Ca peak. The TEM analyses of all synthesized nanoparticles are reported in a previous work [24], this study showed evidence of a pseudo-spherical shape of all nanoparticles and the presence of a silica shell of about 1-2 nm around the magnetic core of MS, MSCa-C and MSCa-H.

3.2 In vitro bioactivity of nanoparticles

First experiment

Pure magnetite (M) samples did not show any morphology ascribable to hydroxyapatite (HAp) precipitates (Figure 2a). Only in some areas of the sample

(evidenced with an arrow in figure 2) EDS analysis (Figure 2b) revealed the presence of Ca and P peaks but in a small amount, which can be due to a few calcium phosphate precipitates.

Silica-coated NPs (MS), after immersion in SBF, showed the typical morphology of *in vitro* grown HAp (Figure 2c). Compositional analysis demonstrated the presence of sharp Ca and P peaks, with a ratio Ca/P of about 1.6, very similar to that of HAp (Figure 2d). MSCa-C NPs did not show the presence of HAp (Figure 2e); compositional analysis of restricted areas (evidenced with arrows) showed evidence of a moderate presence of P, while the Si and Ca peaks originated from the starting material (Figure 2f). The same behavior was observed for MSCa-H NPs; they showed a moderate P peak, but at a morphological level, the presence of similar hydroxyapatite precipitates was not observed (Figure 2g and h).

Second experiment

In the second experiment, powders weren't dried before their immersion in SBF solution to avoid particle agglomeration. In this second experiment, only MS NPs and MSCa-H NPs were investigated on the basis of results obtained in the first study.

The morphology of both tested nanoparticles appeared to have changed after the SBF immersion. A reaction layer that covered the NPs (Figure 3a and d) with the typical structure of the *in vitro* grown HAp was observed (Figure 3b and e). The EDS analysis showed evidence of a large presence of P and Ca together with the material components (Fe, Si, and O). Na and Cl peaks were due to the precipitation of NaCl salt, while Mg and K (SBF components) derived probably from their introduction into the apatite layer (Figure 3c and f). Unlike the first experiment, in this case, calcium

functionalized particles (MSC-H) showed the same behavior as silica-coated NPs; they were covered by a reaction layer, composed mainly of P and Ca (EDS analysis), indicating the bioactive behavior of the sample. This test confirmed the influence of the agglomeration, due to samples preparation, and the exposed surface area in the bioactive mechanism.

On the basis of obtained results, it was decided to include only the silica-coated nanoparticles in the PMMA, since they showed a very promising bioactive behavior, and the addition of calcium in the silica shell did not induce a significant improvement of the bioactivity.

3.3 Nanocomposites characterization

3.3.1 Morphological and compositional characterization of the (S+M) composites obtained with the three different mixing methods.

Morphological and compositional characterization was performed in order to find the best method to synthesize the nanocomposite cement. The mixing sequence was selected on the basis of FESEM-EDS analysis performed on magnetite-containing composite samples (S+M), obtained by the three different mixing sequence methods, as reported in “materials and methods” section.

Method # 1: FESEM and compositional EDS measurements demonstrated the presence of magnetite NPs well dispersed in the polymeric matrix and exposed on cement surface (Figure 4a, b and c).

Method # 2

FESEM characterization showed evidence of only a partial exposure of magnetic nanoparticles (Figure 4d, e and f). At high magnification, the surface of the composite appeared smoother than those obtained with *Method # 1* (Figure 4f) and magnetic NPs were not clearly visible, even if EDS analysis showed evidence of the presence of Fe peak. (Figure 4e).

Method # 3

FESEM-EDS analyses showed evidence of the presence of NPs agglomerates underneath the surface of the cement (Figure 4g, h and i).

3.3.2 Morphological and compositional characterization of the bone cements obtained with the mixing Method # 1 (hand mixing).

The mixing Method # 1 revealed the best results in terms of NPs dispersion and appearance at the surface. So, the comparison between plain Simplex® (S) and the two composites (S+M and S+MS) was performed on specimens obtained with this mixing method containing 10 wt% of NPs.

Figure 5 reports the results obtained using the manual mixing method. The backscattered image of pure Simplex® showed evidence of the PMMA spheres (the black circles in figure 5a). The light emitting white particles refer to the barium sulfate dispersed as the radiopacifier particles in the micrometer size range. A few small barium sulfate agglomerates (marked with circle in figure 5a) were also observed.

The backscattered FESEM image of the composite containing magnetite powder (Figure 5b) revealed almost the same material's structure as that of pure Simplex©. PMMA spheres from the powder were observed as well as barium sulfate and some

agglomerates of magnetite NPs. However, EDS analysis (Figure 5c and d) showed evidence of the presence of magnetite well dispersed NPs along with the agglomerates.

The samples containing silica coated NPs, also revealed the presence of NPs agglomerates (Figure 5e). These samples however also revealed the presence of well dispersed silica coated NPs, confirmed by the EDS analysis, which showed the presence of Si and Fe peaks (Figure 5f, g and h).

3.3.3 Mechanical mixing and its correlation with compressive strength and working time

The correct range of blending speed had to be established since in the literature there was no data on the investigation of the speed of mechanical mixing.

As shown in figure 6, mixing speed had a strong influence on the compression behavior of the material (the line at 70 MPa indicates the limit imposed by the ISO 5833 standard). As can be observed, a low mechanical mixing speed did not allow an adequate compressive strength to be achieved; instead, by mixing at speed ≥ 1000 rpm the compressive strength reached optimal values higher than the limit imposed by the ISO standard.

The speed was chosen to be 1500 rpm on the basis of the obtained results, which allowed a compressive strength similar to the manual mixed cement of about 80 MPa to be attained.

3.3.4 FESEM-EDS characterization of S+M and S+MS composites obtained with mechanical mixing

5 wt% NPs, 1500 rpm mixing

Composite bone cements containing 5 % in weight of NPs and mechanically mixed at 1500 rpm were investigated by means of FESEM-EDS analysis to evaluate the NPs dispersion.

As it can be observed in figure 7, the mechanical stirring and the reduction of the weight percentage of NPs provide a better dispersions of the nanoparticles in the polymer matrix. NP agglomerates were observed in only a few regions of the samples (Figure 7b, c); however, these agglomerates were much smaller than clusters observed using 10 wt% of NPs and manually mixed. Compositional analysis of a wide area without agglomerates (Figure 10d and f) showed the presence of peaks characteristics of NPs, showing evidence of a uniform dispersion of NPs in the polymeric matrix.

10 wt% NPs, 1500 rpm mixing

Composite bone cements containing 10 wt% of magnetite and silica coated magnetite nanoparticles, prepared using a mixing speed of 1500 rpm, were characterized with FESEM-EDS (Figure 8).

As previously observed the high speed method improves the dispersion of the nanoparticles and a reduction in the size of clusters. Also, in this case, very few NPs agglomerates were observed and EDS analysis showed the presence of NPs and their uniform dispersion in the PMMA matrix.

3.3.5. Density measurements

The obtained specimens were investigated after three days and the relative density was calculated by *Mohr's balance.* This test revealed no differences in cement's density

(Table 2), so the optimized mechanical mixing allowed cement with adequate mechanical properties to be prepared.

3.3.6 Compression test results

As reported in literature [35], the addition of hard particles, such as magnetite, in a glassy polymer can decrease the mechanical properties of the composite creating a larger number of crack initiation sites. Yield and ultimate load were determined as previously described for Surgical Simplex© P (S), S+M hand mixed 5 wt%, S+M mechanically mixed 5 and 10 wt% S+MS hand mixed 5 and S+MS mechanically mixed 5 and 10 wt%,.

As can be observed in figure 9, the increase of NPs fraction lead to a further reduction of the mechanical properties.

Moreover, figure 9 demonstrated that the introduction of the silica shell decreased the mechanical strength of the composite.

3.3.7 Composite cement bioactivity

- 5 wt% and 10 wt% hand mixed

FESEM-EDS analyses of composite bone cements containing 5 and 10 wt % of NPs manually mixed after 7 and 28 days of SBF immersion are reported in figure 10.

On all sample surfaces, it was possible to observe the presence of some precipitates; EDS analyses performed on these precipitates showed evidence of (in comparison with the unsoaked samples) a clear decrease of Si peak and an increase of Ca and P peaks, probably due to the nucleation of hydroxyapatite precursors or its precursor. After 28 days of SBF treatment on composite cement surface containing 10 wt% of silica coated

magnetic NPs some precipitates were observed with the characteristic morphology of HAp (Figure 10l-n)

- 5 wt% and 10 wt% mechanical mixed at 1500 rpm

Figure 11 shows the morphological and compositional analyses performed after 7, 14 and 28 days of SBF immersion of composite bone cements mechanically mixed containing 5 and 10 wt% of silica-coated magnetite NPs. After 7 days of SBF treatment a few precipitates rich in Ca were visible in figures 11a-c and 11l-n, both for 5 and 10 wt% of magnetic nanoparticles containing cements. After 14 and 28 days (Figure 11d-f and g-I 5 wt%, Figure 11o-q and r-t 10 wt%), it was possible to distinguish the typical structure of hydroxyapatite nucleated on the surface of samples. As confirmation, the compositional analysis of the "*cauliflower*" area presents a sharp peak of calcium and phosphorous. Moreover, after 28 days of immersion the ratio Ca/P (1.77 for 5 wt % and 1.68 for 10 wt %) was comparable with the theoretical ratio of HAp (1.71).

For all samples (5 and 10 wt%, mechanical and hand mixed) the pH remained within the physiological range of 7 to 7.8.

3.3.8 Magnetic characterization of composite bone cements

The hysteresis cycles for composite cements containing magnetite NPs and magnetite-silica NPs up to 800 kA/m are shown in figure 12. The obtained curves exhibited the typical behavior of a superparamagnetic material: the coercive field and remanence magnetization are negligible at room temperature. The saturation magnetization (Ms) of S+M sample reached about 30 Am^2/Kg, while Ms of S+MS sample was around 20

Am^2/Kg. As previously reported[21], there was no change in the magnetic properties of both composites regardless of the weight of the silica coating.

4. Discussion

The main goal of the project was to impart bioactive and magnetic properties to the PMMA-based bone cement, generally used as filler after bone tumor removal. In the literature, a few studies reported the use of magnetic nanoparticles embedded in a polymeric matrix to treat metastatic bone tumor [15,36,37] by means of hyperthermia. While, on the basis of the authors knowledge, only a few papers considered composite bone cements, which were simultaneously bioactive and magnetic [19-21] and most of them incorporated glass-ceramic microparticles in the polymeric matrix. In this paper, a novel approach was used to develop a composite bone cement containing magnetic nanoparticles useful for hyperthermic treatment and at the same time be able to integrate with host tissue. Magnetite-based NPs, synthesized by means of co-precipitation process, were coated with a thin layer (1-2 nm) of silica, normally used to protect NPs and improve NPs dispersion. In this case, for the first time on the basis of authors knowledge, the role of silica shell in the bioactivity mechanism was investigated and compared with a silica shell-doped with Ca ions. A few authors studied the ability of silica to promote the formation and precipitation of hydroxyapatite [38]; Nayak et al., for example, showed the hydroxyapatite precipitation on amorphous silica after a few days in SBF; they reported that the mechanism of HAp formation involves the presence of Si-OH group on silica surface, which in SBF solution (pH 7.4) form a negatively charges surface:

$\equiv SiOH + OH^- \rightarrow SiO^- + H_2O$

Subsequently, the Ca^{+2} and the PO_4^{3-} group migrates to the surface, forming $Ca–PO_4^{3-}$ amorphous precipitates, which crystallize and form a HAp layer. Moreover, it was reported that Si-OH groups provide favorable sites for apatite nucleation since they promote the adsorption of Ca^{2+} ion and phosphate ion on the surface [39]. Moreover, Sanchez et al. [22], investigated the bioactivity of Fe-Ga nanoparticles produced by sol-gel. However, they induce the NPs bioactivity by immersing samples in SBF solution in the presence of a wollastonite disk, thus realizing a biomimetic method.

The bioactivity test in SBF solution of MS and MSC NPs confirmed the ability of hydrated silica to induce the precipitation of HAp. In the first test, only MS nanoparticles were able to significantly promote the formation of calcium-phosphate precipitates on their surface, while M and MSC NPs did not show the presence of HAp. The second test, performed by preventing NP agglomeration, showed evidence that the agglomeration state also influenced the particles reactivity, since MSC NPs were also able to promote HAp formation. However, the presence of Ca seemed to not influence or accelerate HAp formation. On the basis of these results, only MS NPs were used to synthesize composite PMMA-based bone cement.

Then, the work focused on the method to disperse magnetic nanoparticles in the cement without change their features and to verify the composite cement properties. Magnetic nanoparticles have the tendency to agglomerate in clusters that could reduce cement's mechanical properties and could make it undesirable to use nano-sized particles.

From a mechanical point of view, both the mixing methods and the filler percentage can influence the strength of composite [35]. In this work, a comparison between the

mechanical and manual mixing (both using vacuum) was estimated: in terms of compression strength. An appropriate speed of mechanical mixing allows a slightly higher compression strength to be attained, using a filler load of 5 wt%. As expected, the mechanical properties decreased just below the limit imposed by ISO standard (70 MPa) by increasing the amount of NPs. The graph of figure 9 also shows that by introducing 5 wt% of NPs, the presence of silica coating appears to influence the mechanical strength, because probably it changes the properties at the interface. This reduction was not observed in the composites containing 10 wt% of NPs, in which the compression strength seems most likely influenced by the amount of NPs. In fact, the parameters that can influence the mechanical strength of the composite are: i) the method of mixing, ii) the amount of the NPs and the properties at the interface NPs/cement. For composites containing 5% of NPs, a decrease of strength for samples containing magnetite-silica (MS) NPs was observed; while they noticed a comparable strength for samples containing 10% of magnetite (M) and MS NPs. Moreover, the strength values of 10% containing samples are comparable with values obtained with 5% MS-containing composites (both manually and mechanically mixed). Therefore, it can be supposed that up to 5% of NPs the presence of silica coating appears to be the key factor that influence the mechanical strength, while introducing 10% of NPs the mechanical strength seems to be more influenced by the amount of NPs rather than by the silica coating.

The *in vitro* bioactivity test of composites showed a delay of HAp formation for cements containing manually mixed NPs, since precipitates rich in Ca and P with the typical morphology of *in vitro* grown HAp were observed only after 28 days of immersion in SBF. Whereas, the surface of composite bone cement showed

precipitates of Ca and P having the HAp morphology within 14 days of SBF treatment (especially for cements containing 10 wt% of NPs) when the mechanical mixing method was used.

This indicates that mechanical mixing effectively improves the dispersion of NPs and so increase NPs surface exposed to biological fluid, thus improving the bioactive behavior of the composite bone cement. Simultaneously, mechanically mixed composite bone cements containing 5 wt% NPs showed a superparamagnetic behavior and magnetization useful for use in hyperthermia treatment, in agreement with observations by other authors [40]. Therefore, the mechanical incorporation of bioactive silica-coated magnetic NPs (MS – 5 wt%) in the PMMA-based bone cement is a promising composite bone cement, both magnetic and bioactive, and useful for the hyperthermia treatment of cancer while simultaneously be able to integrate with peri-cement bone tissue.

Conclusions

This work demonstrated for the first time the ability of silica-coated magnetite-based NPs to induce the precipitation of HAp when immersed in SBF solution. These bioactive and magnetic NPs were then used as a filler for PMMA-based bone cements. Composite bone cements were synthesized using different amounts (5 and 10 wt%) of bioactive and magnetic NPs and using both manual and mechanical mixing methods. The obtained results showed that the mechanical mixing allowed a better dispersion of NPs to be achieved in the polymeric matrix than the manual method. In general, an increase of the NPs amount reduced the mechanical properties, while the bioactivity

and the superparamagnetic properties of the composites were maintained also introducing 5 wt% of NPs.

In conclusion, silica coated-magnetic NPs proved to be a promising filler to impart bioactive and magnetic properties to PMMA-based bone cements, thus obtaining multifunctional stimuli-responsive composite bone cements for the treatment of bone tumors and associated complications.

Funding

This research did not receive any specific grant from funding agencies in the public, commercial, or not-for-profit sectors.

References

[1] Malawer, M.M. Helman, L.J. O'Sullivan, B. Sarcomas of bone. In: DeVita, V.T. Jr; Lawrence, T.S.; Rosenberg, S.A. Cancer: Principles and Practice of Oncology. 9th ed. Philadelphia, Pa: Lippincott Williams & Wilkins, 2011; p 1578-1609.

[2] Siegel, R. Naishadham, D. Jemal, A. Cancer statistics, 2012. CA Cancer J Clin. 62(1) (2012) 10-29. doi: 10.3322/caac.20138.

[3] Dougan, M. Dranoff, G. Immune Therapy for Cancer. Annu. Rev. Immunol. 27 (2009) 83-117. doi: 10.1146/annurev.immunol.021908.132544.

[4] Firczuk, M. Winiarska, M. Szokalska, A. Jodlowska, M. Swiech, M. Bojarczuk, K. Salwa, P. Nowis D. Approaches to improve photodynamic therapy of cancer. Front. Biosci. 16 (2011) 208-224, DOI: 10.2741/3684.

[5] http://www.esho.info/professionals/hyperthermia/description/index.html, visited 02/07/2018.

[6] Cheung, A.Y. Neyzari, A. Deep local hyperthermia for cancer therapy: external electromagnetic and ultrasound techniques. Cancer Res 44 (1984) 4736s-4744s. https://www.ncbi.nlm.nih.gov/pubmed/6467228

[7] Mohamed, M. Borchard, G. Jordan, J. In situ forming implants for local chemotherapy and hyperthermia of bone tumors. J. Drug Del. Sci. Tech. 22 (5) (2012) 393-408. https://archive-ouverte.unige.ch/unige:24338

[8] Vogt, S. Büchner, H. Polymethylmethacrylate bone cement composition for controlled hyperthermia treatment. Patent US2010/0160483 A1.

[9] Kawashita, M. Kawamura, K. Li, Z. PMMA-based bone cements containing magnetite particles for the hyperthermia of cancer. Acta Biomater. 6 (2010) 3187–3192, doi: 10.1016/j.actbio.2010.02.047.

[10] Challa, S.S.R.K. Faruq, M. Magnetic nanomaterials for hyperthermia-based therapy and controlled drug delivery. Advanced Drug Delivery Reviews 63 (2011) 789–808. https://doi.org/10.1016/j.addr.2011.03.008.

[11] Roca, A.G. Gutiérrez, L. Gavilán, H. Fortes Brollo, M.E. , Veintemillas-Verdaguer, S. del Puerto Morales, M. Design strategies for shape-controlled magnetic iron oxide nanoparticles, Adv. Drug Deliv. Rev. 138 (2019) 68-104. https://doi.org/10.1016/j.addr.2018.12.008.

[12] Miola, M. Pakzad, Y. Banijamali, S. Kargozar, S. Vitale-Brovarone, C. Yazdanpanah, A. Bretcanu, O.Ramedani, A. Vernè, E. Mozafari, M. Glass-ceramics for cancer treatment: So close, or yet so far? Acta Biomaterialia 83 (2019) 55-70. https://doi.org/10.1016/j.actbio.2018.11.013.

[13] Arora, M. Chan, E.K. Gupta, S. Diwan, A.D. Polymethylmethacrylate bone cements and additives: A review of the literature. World J. Orthop. 4(2) (2013) 67-74, doi: 10.5312/wjo.v4.i2.67.

[14] Shinzato, S. Kobayashi, M. Mousa, W.F. Kamimura, M. Neo, M. Kitamura, Y. Kokubo, T. Nakamura, T. Bioactive polymethyl methacrylate-based bone cement: Comparison of glass beads, apatite- and wollastonite-containing glass–ceramic, and hydroxyapatite fillers on mechanical and biological properties. 51(2) (2000) 258-272, DOI:10.1002/(SICI)1097-4636(200008)51:2<258::AID-JBM15>3.0.CO;2-S

[15] Li, Z. Kawamura, K. Kawashita, M. Kudo, T. Kanetaka, H. Hiraoka, M. In vitro assessment of poly(methylmethacrylate)-based bone cement containing magnetite nanoparticles for hyperthermia treatment of bone tumor. J Biomed Mater Res A. 100(10) (2012) 2537-2345, doi: 10.1002/jbm.a.34185.

[16] Harabech, M. Kiselovs, N.R. Maenhoudt, W. Crevecoeur, G. Van Roost, D. Dupré, L. Experimental ex-vivo validation of PMMA-based bone cements loaded with magnetic nanoparticles enabling hyperthermia of metastatic bone tumors. AIP Advances 7 (2016) 056704, DOI: 10.1063/1.4973499.

[17] Tanga, Z. Wang, X. Panc, L. Hu, Y. Wu, Y. Zhang, J. Cuid, S. Kang, K. Tang, J. Preparation and Characterization of PMMA-based Cements Containing Magnetic Nanoparticles for the Magnetic Hyperthermia. Advanced Materials Research Online 647 (2013) 155-159, doi.org/10.4028/www.scientific.net/AMR.647.155

[18] Takegami, K. Sano, T. Wakabayashi, H. Sonoda, J. Yamazaki, T. Morita, S. Shibuya, T. Uchida, A. New ferromagnetic bone cement for local hyperthermia. J Biomed Mater Res (Appl Biomater) 43 (1998) 210–214, doi:10.1002/(SICI)1097-4636(199822)43:2<210::AID-JBM16>3.0.CO;2-L.

[19] Miola, M. Laviano, F. Gerbaldo, R. Bruno, M. Lombardi, A. Cochis, A. Rimondini, L. Verné, E. Composite bone cements for hyperthermia: modeling and characterization of magnetic, calorimetric and in vitro heating properties. Ceramics International 43 (2017) 4831–4840, doi:10.1016/j.ceramint.2016.12.049.

[20] Verné, E. Bruno, M. Miola, M. Maina, G. Bianco, C. Cochis, A. Rimondini, L. Composite bone cements loaded with a bioactive and ferrimagnetic glass-ceramic: Leaching, bioactivity and cytocompatibility. Mat. Sci. Eng, C: Mat. for Biol. App. 53 (2015) 95-103, doi: 10.1016/j.msec.2015.03.039.

[21] Bruno, M. Miola, M. Bretcanu, O. Vitale-Brovarone, C. Gerbaldo, R. Laviano, F. Verné, E. Composite bone cements loaded with a bioactive and ferrimagnetic glass-ceramic. Part I: morphological, mechanical and calorimetric characterization. J. Biomater. App. 29(2) (2014) 254-267, DOI: 10.1177/0885328214521847.

[22] Sánchez, J. Cortés-Hernández, D.A. Escobedo-Bocardo, J.C. Jasso-Terán, R.A. Zugasti-Cruz, A. Bioactive magnetic nanoparticles of Fe-Ga synthesized by sol-gel for their potential use in hyperthermia treatment. J Mater Sci Mater Med. 25(10) (2014) 2237-2242. doi: 10.1007/s10856-014-5197-1.

[23] Li, Z. Kawashita, M. Araki, N. Mitsumori, M. Hiraokc, M. Doi, M. Magnetite nanoparticles with high heating efficiencies for application in the hyperthermia of cancer. Mat. Sci. Eng. C 30 (2010) 990–996, doi :10.1016/j.msec.2010.04.016.

[24] Borroni, E. Miola, M. Ferraris, S. Ricci, M. Žužek Rožman, K. Kostevšek, N. Catizone, A. Rimondini, L. Prat, M. Verné E. Follenzi, A. Tumor Targeting by Lentiviral Vectors Combined with Magnetic Nanoparticles in Mice, Acta Biomaterialia 59 (2017) 303-316. doi: 10.1016/j.actbio.2017.07.007.

[25] Maity, D. Agrawal, D.C. Synthesis of iron oxide nanoparticles under oxidizing environment and their stabilization in aqueous and non-aqueous media. J. Magnetism and Magnetic Mat. 308 (1) (2007) 46-55. doi:10.1016/j.jmmm.2006.05.001.

[26] Yallapu, M.M. Othman, S.F. Curtis, E.T. Gupta, B.K. Jaggi, M. Chauhan, S.C. Multi-functional magnetic nanoparticles for magnetic resonance imaging and cancer therapy. Biomaterials 32 (7) (2011) 1890-1905. doi: 10.1016/j.biomaterials.2010.11.028.

[27] Campelj, S. Makovec, D. Drofenik, M. Preparation and properties of water-based magnetic fluids. J Phys Condens Matter. 20(20) (2008) 204101. doi: 10.1088/0953-8984/20/20/204101.

[28] Deng, Y.H. Wang, C.C. Hu, J.H. Yang, W.L. Fu, S.K. Investigation of formation of silica-coated magnetite nanoparticles via sol-gel approach. Colloids Surfaces A Physicochem Eng Asp. 262(1-3) (2005) 87-93. http://www.meplab.fudan.edu.cn/infonet/assays/2005/Investigation%20of%20formation%20of%20silica-coated%20magnetite%20nanoparticles%20via%20sol-gel%20approach.pdf

[29] Ohtsuki, C. Kokubo, T. Yamamuro, T. Mechanism of apatite formation on cao-SiO_2-P_2O_5 glasses in a simulated body-fluid. J. Non- Cryst. Solids 143 (1992) 84-92. DOI: 10.1016/S0022-3093(05)80556-3.

[30] Ohtsuki, C. Kamitakahara, M. Miyazaki, T. Bioactive ceramic-based materials with designed reactivity for bone tissue regeneration, J. R. Soc. Interface. 6 (2009) S349-60. doi:10.1098/rsif.2008.0419.focus.

[31] Kalska-Szostko, B. Wykowska, U.;Satula, D. Nordblad Beilstein J.P. Thermal treatment of magnetite nanoparticles. Nanotechnol. 6 (2015)1385–1396. doi:10.3762/bjnano.6.143

[32] Kokubo, T. Takadama, H. How useful is SBF in predicting in vivo bone bioactivity? Biomat. 27 (2006) 2907–2915. doi: 10.1016/j.biomaterials.2006.01.017.

[33] Vaishya, R. Chauhan, M. Vaish, A. Bone cement. J Clin Orthop Trauma. 4(4) (2013) 157–163. doi: 10.1016/j.jcot.2013.11.005.

[34] International standard ISO 5833 “Implants for surgery — Acrylic resin cements” Second edition 2002-05-01.

[35] Rentería-Zamarrón, D. Cortés-Hernández, D.A. Bretado-Aragón, L. Ortega-Lara, W. Mechanical properties and apatite-forming ability of PMMA bone cements. Materials & Design. 30(8) (2009) 3318-3324. DOI: 10/1016/j.matdes.2008.11.024

[36] Harabech, M. Kiselovs, N.R. Maenhoudt, W. Crevecoeur, J. Van Roost, D. Experimental ex-vivo validation of PMMA-based bone cements loaded with magnetic nanoparticles enabling hyperthermia of metastatic bone tumors. AIP Advances 7 (2017) 056704. doi: 10.1063/1.4973499.

[37] Tang, Z. Wang, X. Pan, l. Hu, Y. Wu, Y. Zhang, J. Cui, S. Kang, J. Tang, J. Preparation and Characterization of PMMA-based Cements Containing Magnetic Nanoparticles for the Magnetic Hyperthermia. Advanced Materials Research Online: 647 (2013) 155-161, doi:10.4028/www.scientific.net/AMR.647.155.

[38] Nayak, J. P. Bera, J. Bioactivity Characterization of Amorphous Silica Ceramics Derived from Rice Husk Ash. Silicon, 4 (2012) 57. Doi:10.1007/s12633-010-9058-3

[39] Vallés Lluch, A. Gallego Ferrer, G. Monleón Pradas, M. Biomimetic apatite coating on P(EMA-co-HEA)/SiO2 hybrid nanocomposites. Polymer, 50 (2009) 2874–2884. DOI: 10.1016/j.polymer.2009.04.022.

[40] Li, Z. Kawamura, K. Kawashita, M. Kudo, T. Kanetaka, H. Hiraoka, M. In vitro assessment of poly(methylmethacrylate)-based bone cement containing magnetite

nanoparticles for hyperthermia treatment of bone tumor. J Biomed Mater Res A. 100(10) 2012 2537-2545, doi: 10.1002/jbm.a.34185.

Captions

Figure 1: picture of magnetic nanoparticles (a), STEM and EDS analyses of M (b, d) and MS (c, e) and MSC-H (f) NPs.

Figure 2 FESEM-EDS analysis of M (a-c), MS (d-f), MSCa-C (g-i) and MSC-H (l-n) after SBF immersion, first experiment.

Figure 3: FESEM-EDS analyses of silica coated magnetite (MS, a ,b, c, and d) and silica-calcium hydroxide (MSC-H) coated magnetite (e, f g and h) after SBF immersion, second experiment.

Figure 4: FESEM-EDS analysis of composite bone cement prepared with three different methods: (a-c) method #1, (d-f) method #2, (g-i) method #3.

Figure 5: FESEM-EDS analysis of composite bone cements. Pure Simplex© P (a), magnetite containing cement (b, c and d), magnetite-silica containing cement (e, f, g and h)

Figure 6: compressive strength vs. speed of pure Simplex© P cement.

Figure 7: FESEM-EDS analysis of Simplex©+5 wt % magnetite (a-d) and Simplex© +5 wt % silica-coated magnetite (e, f) using a mixing speed of 1500rpm.

Figure 8**:** FESEM-EDS analysis of Simplex© +10 wt % magnetite (a, b) and Simplex©+10 wt % silica-coated magnetite (c, d) using a mixing speed of 1500rpm.

Figure 9: compressive strengths of composite bone cement (2% offset load)

Figure 10: FESEM-EDS analyses of composite bone cements containing 5 (a-f) and 10 (g-n) wt% of silica-coated magnetite NPs manually mixed after 7 (a-c, g-i) and 28 (e-f, l-n) days of SBF immersion

Figure 11: FESEM-EDS analyses of composite bone cements containing 5 and 10 wt% of silica-coated magnetite NPs mechanically mixed after 7, 14 and 28 days of SBF immersion

Figure 12: Hysteresis cycles of S+M and S+MS composite bone cement containing 5 wt% NPs

Tables

Table 1: samples acronyms, composition and mixing method.

Bone cement (acronym)	**Hand mixing**	**Mechanical mixing**	**wt% of nanoparticles**
Simplex© P (S)	X	X	0
Simplex© P + magnetite (S+M)	X	X	5, 10
Simplex© P+ magnetite-silica (S+MS)	X	X	5, 10

Table 2: average relative density evaluation of Simplex© P cement, hand and mechanically mixed.

Sample	**Average relative density**	**St. deviation**

Hand mixed	49.2	2.7
Mechanical mixed	46.0	1.3

Figure1

Click here to download high resolution image

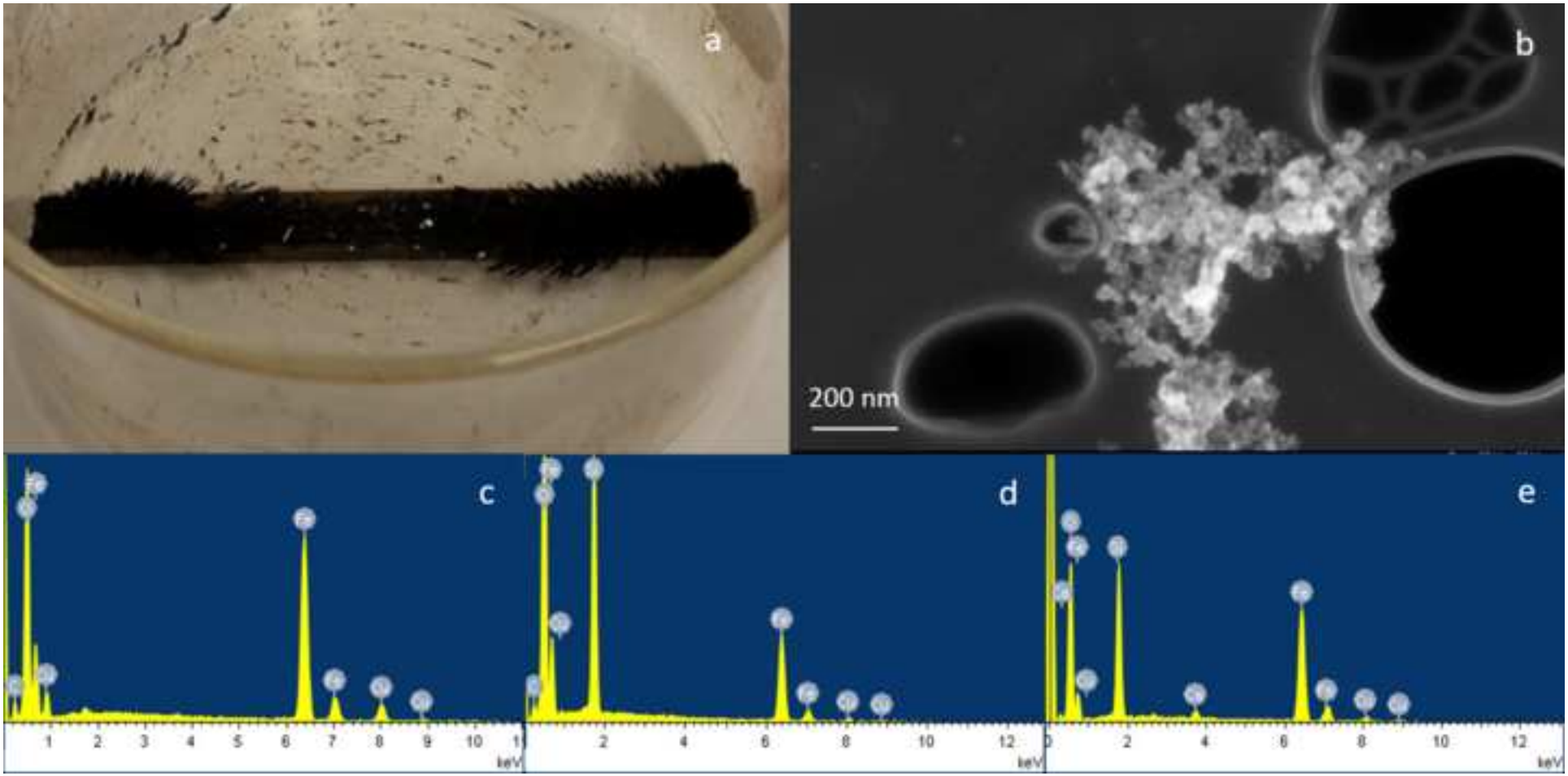

Figure2

Click here to download high resolution image

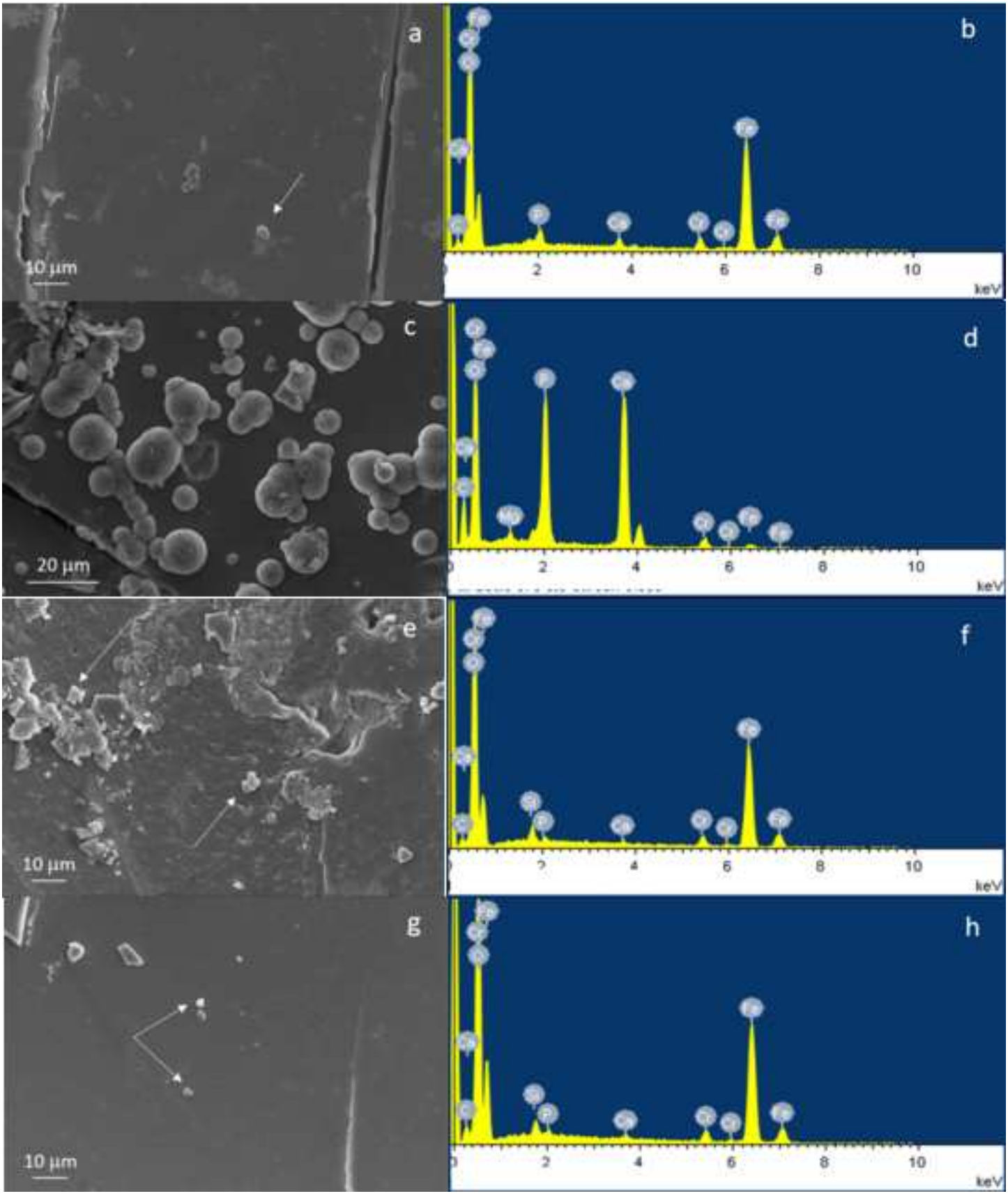

Figure3

Click here to download high resolution image

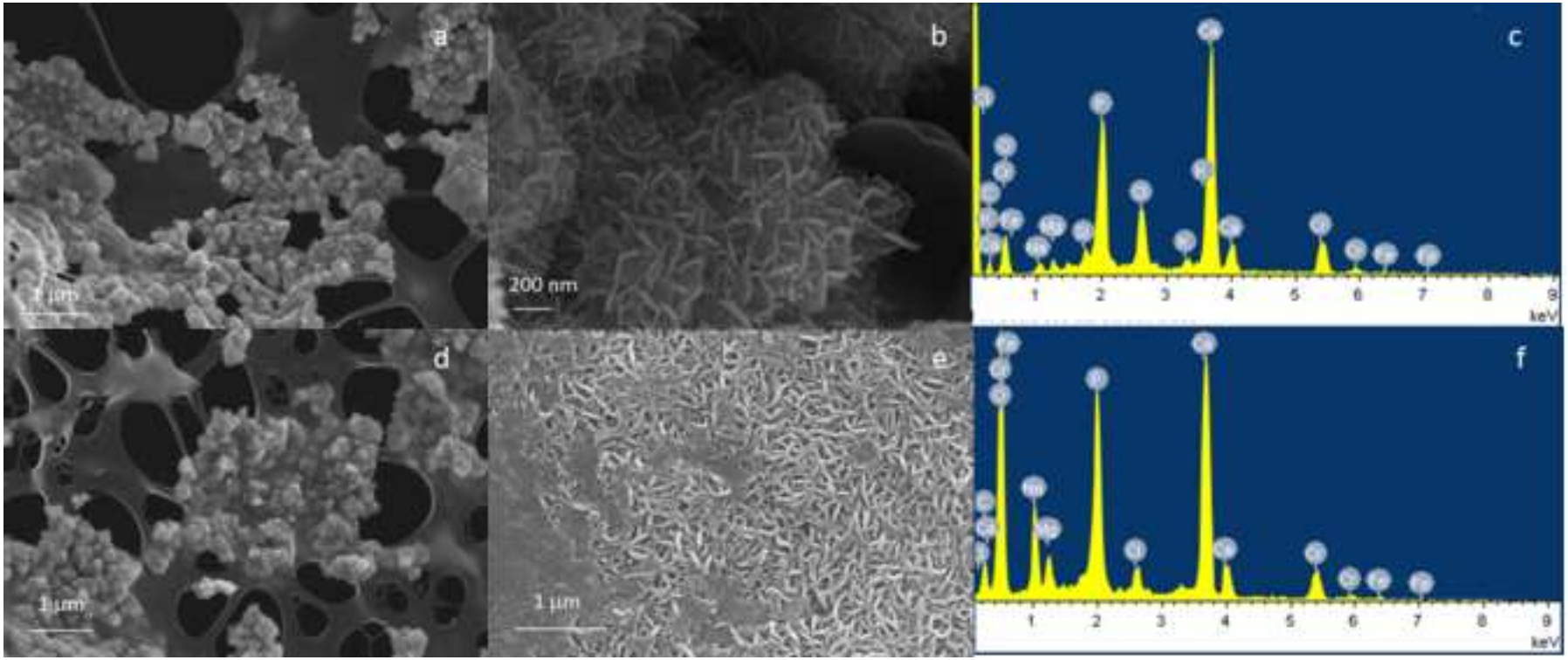

Figure4

Click here to download high resolution image

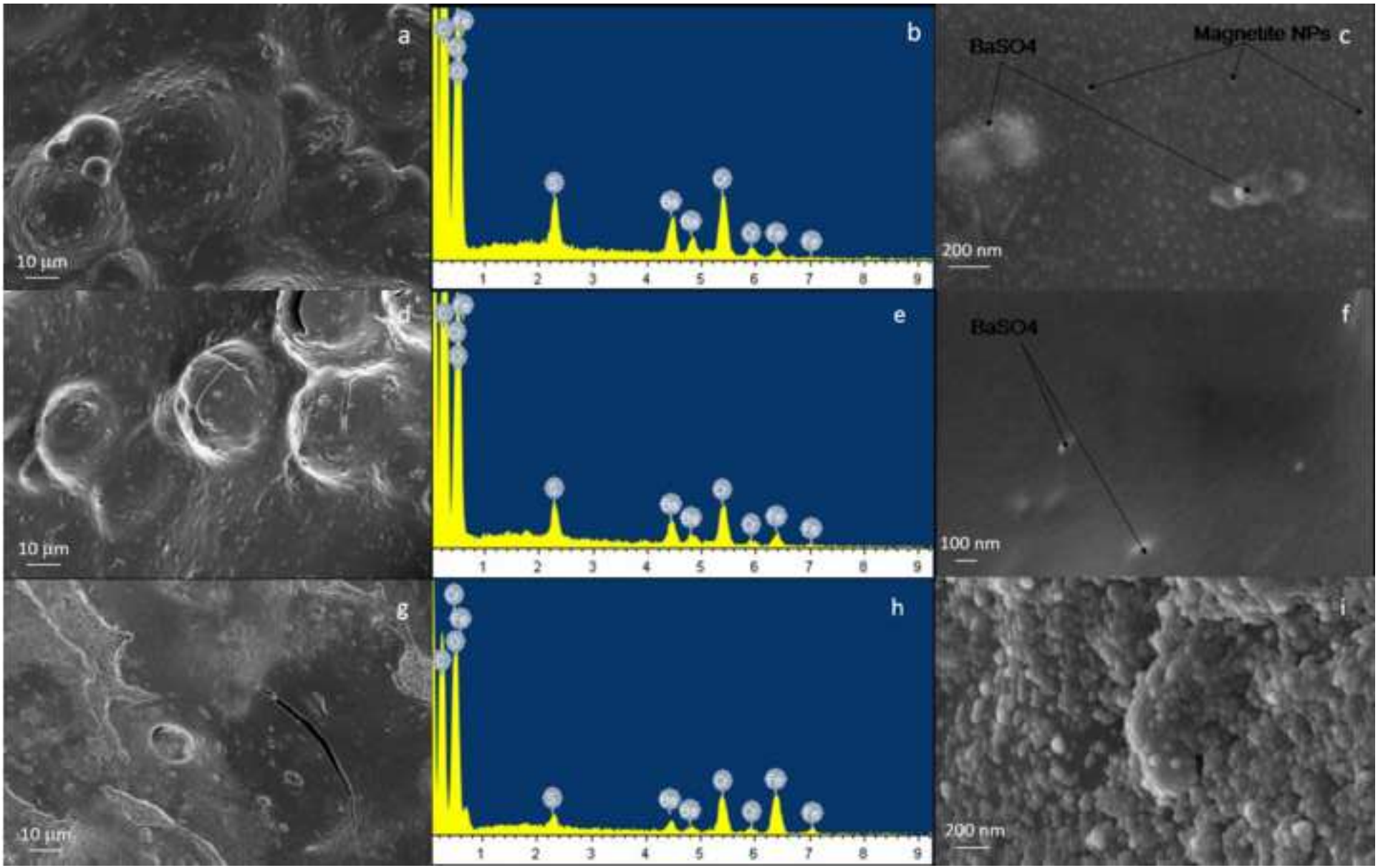

Figure5

Click here to download high resolution image

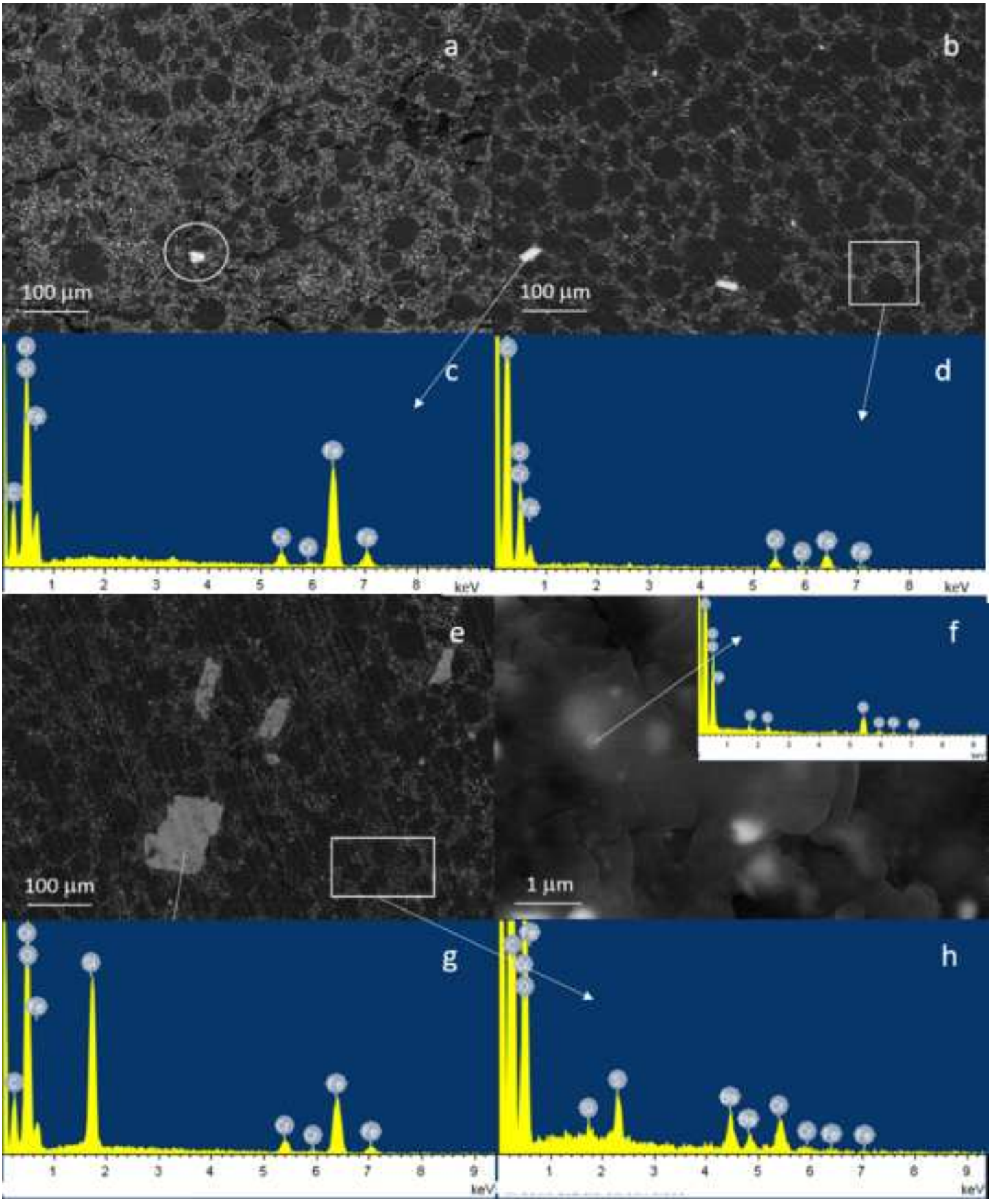

Figure6
Click here to download high resolution image

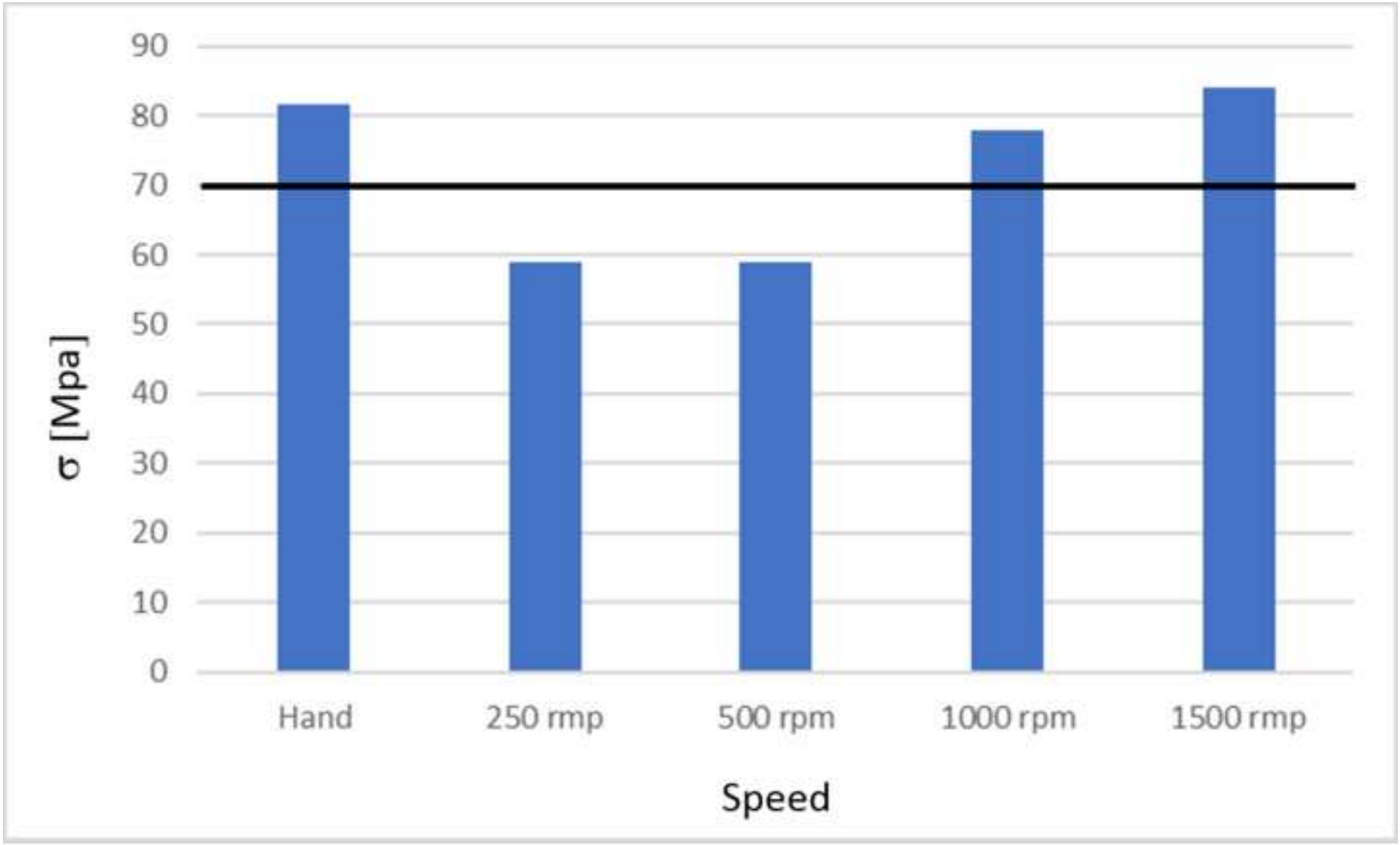

Figure7

Click here to download high resolution image

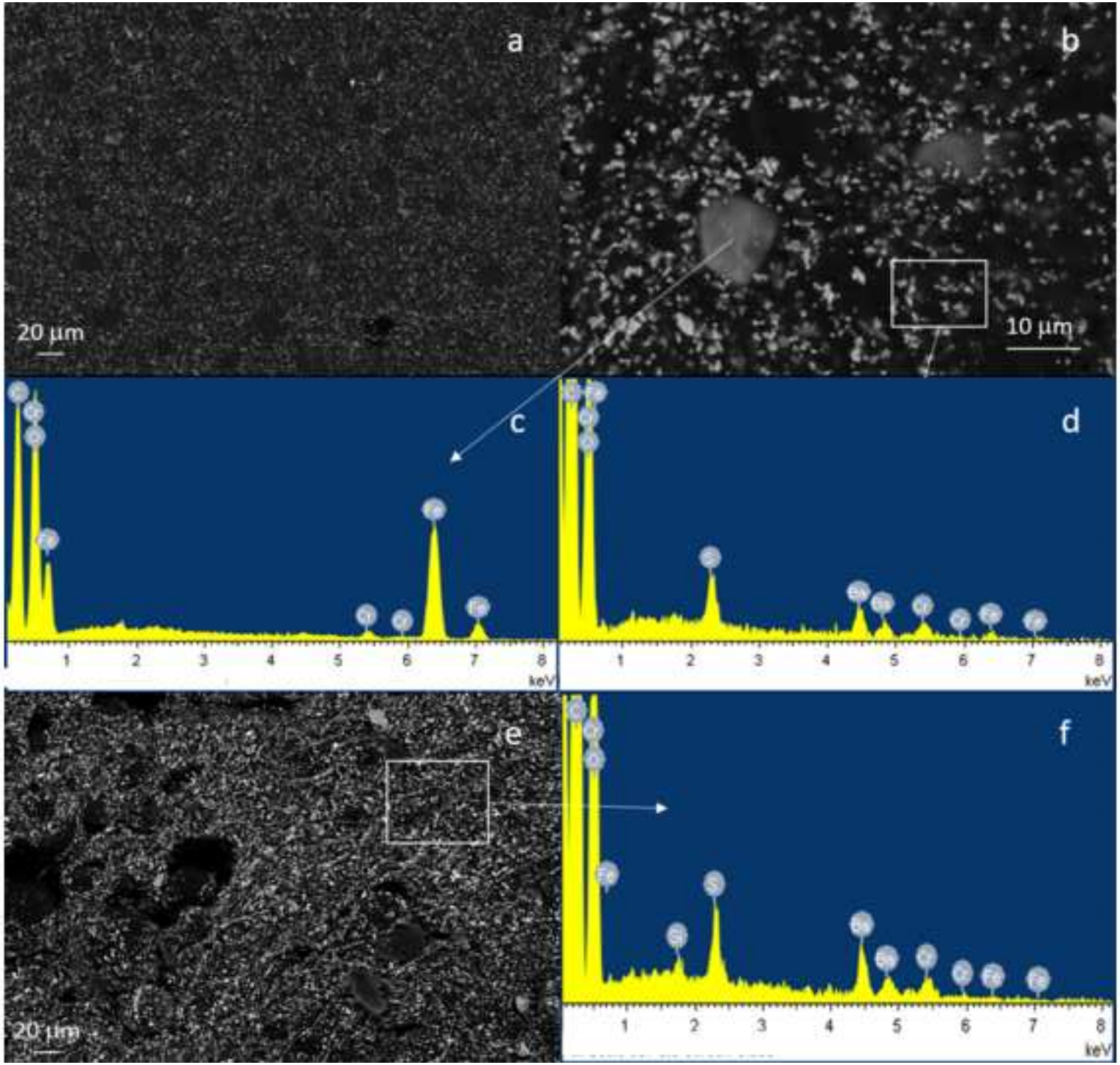

Figure8

Click here to download high resolution image

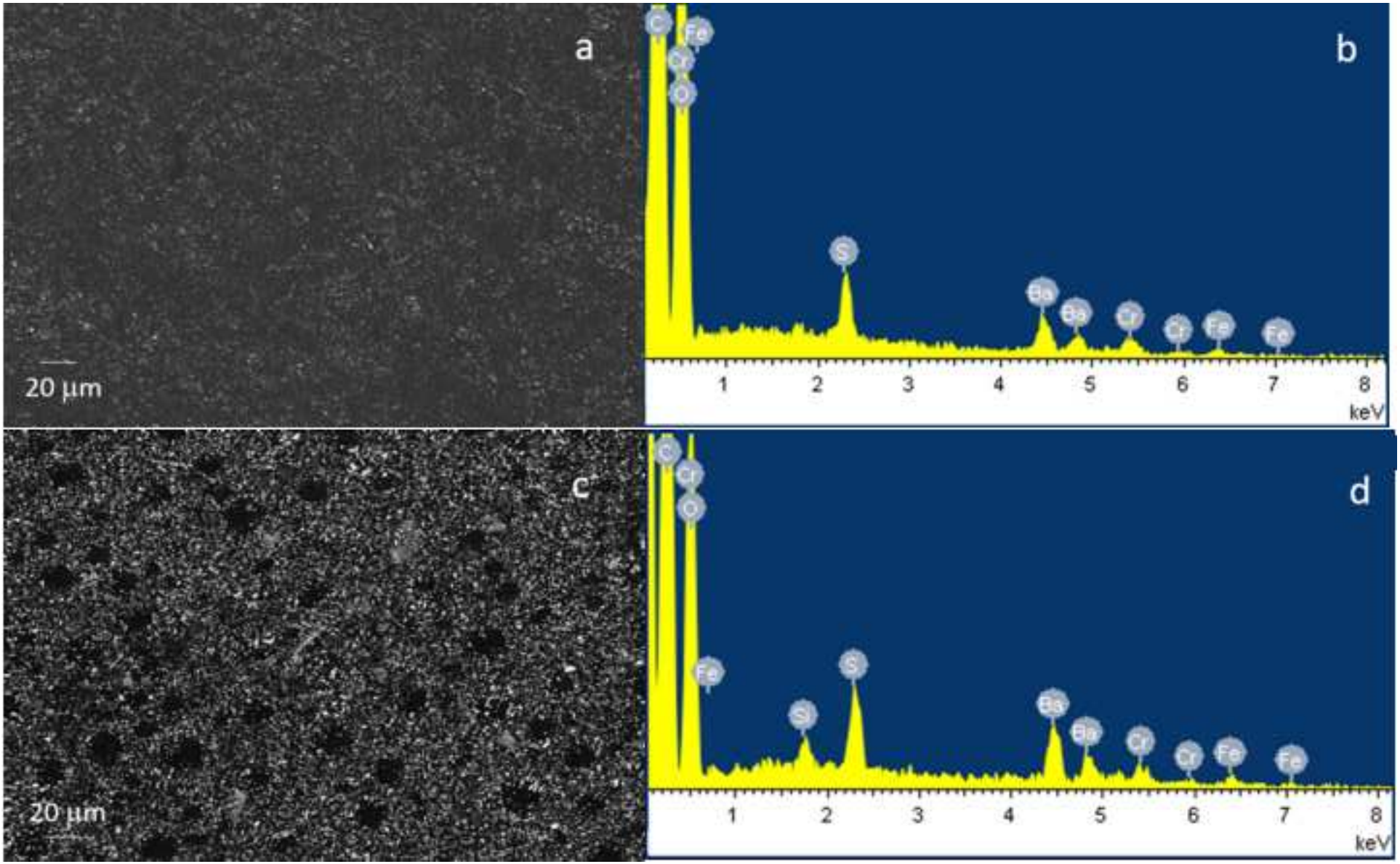

Figure9

Click here to download high resolution image

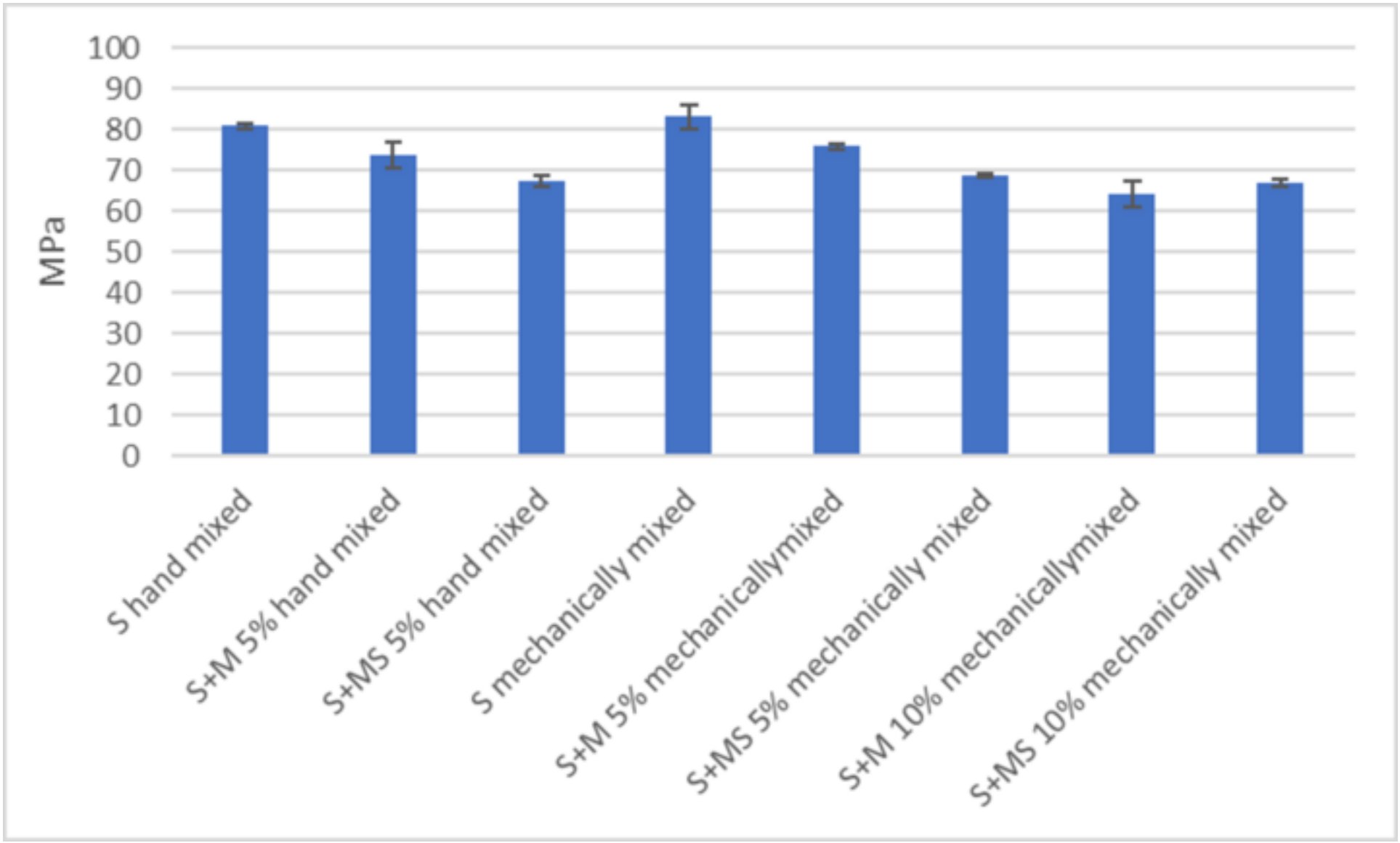

Figure10

Click here to download high resolution image

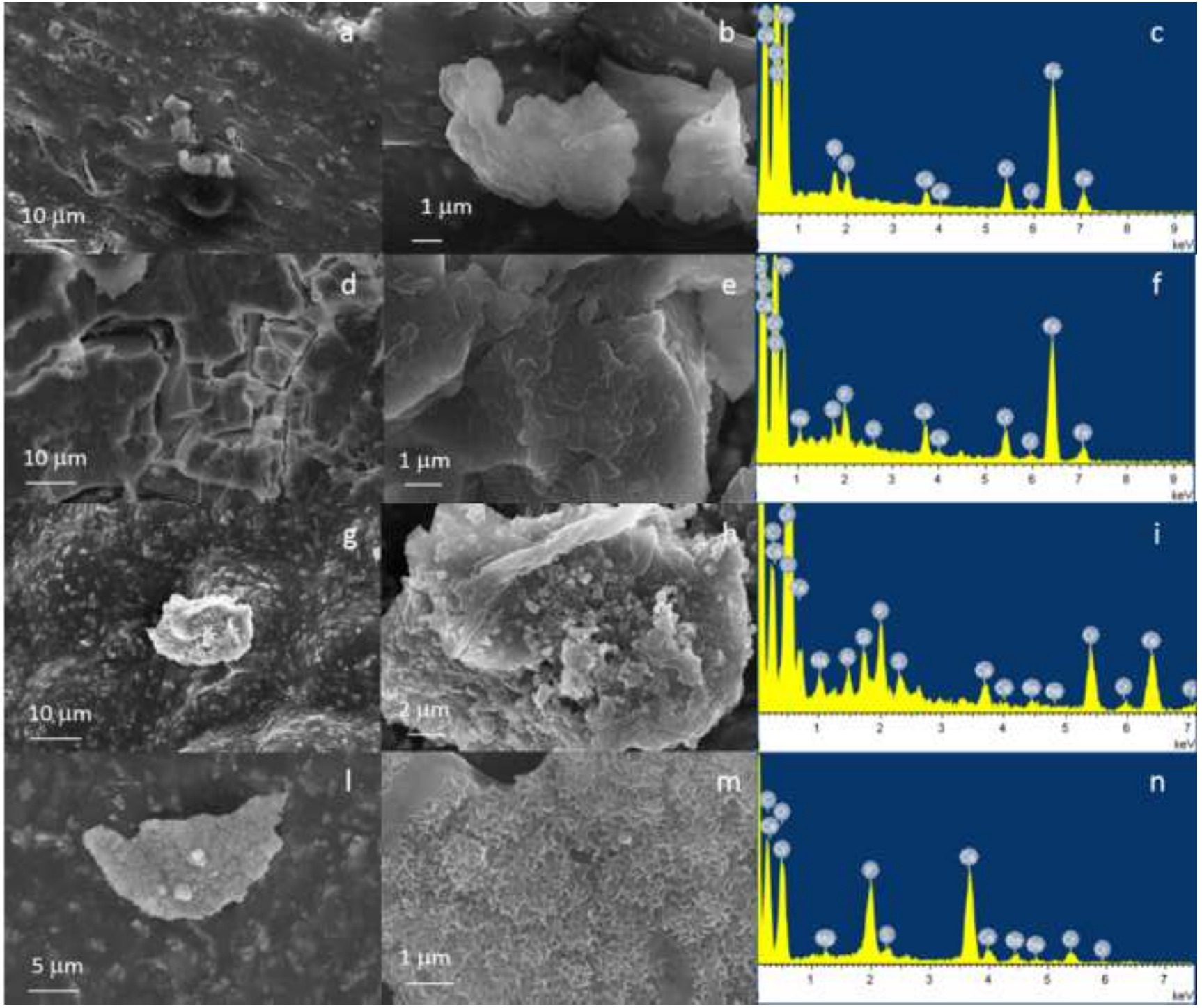

Figure11

Click here to download high resolution image

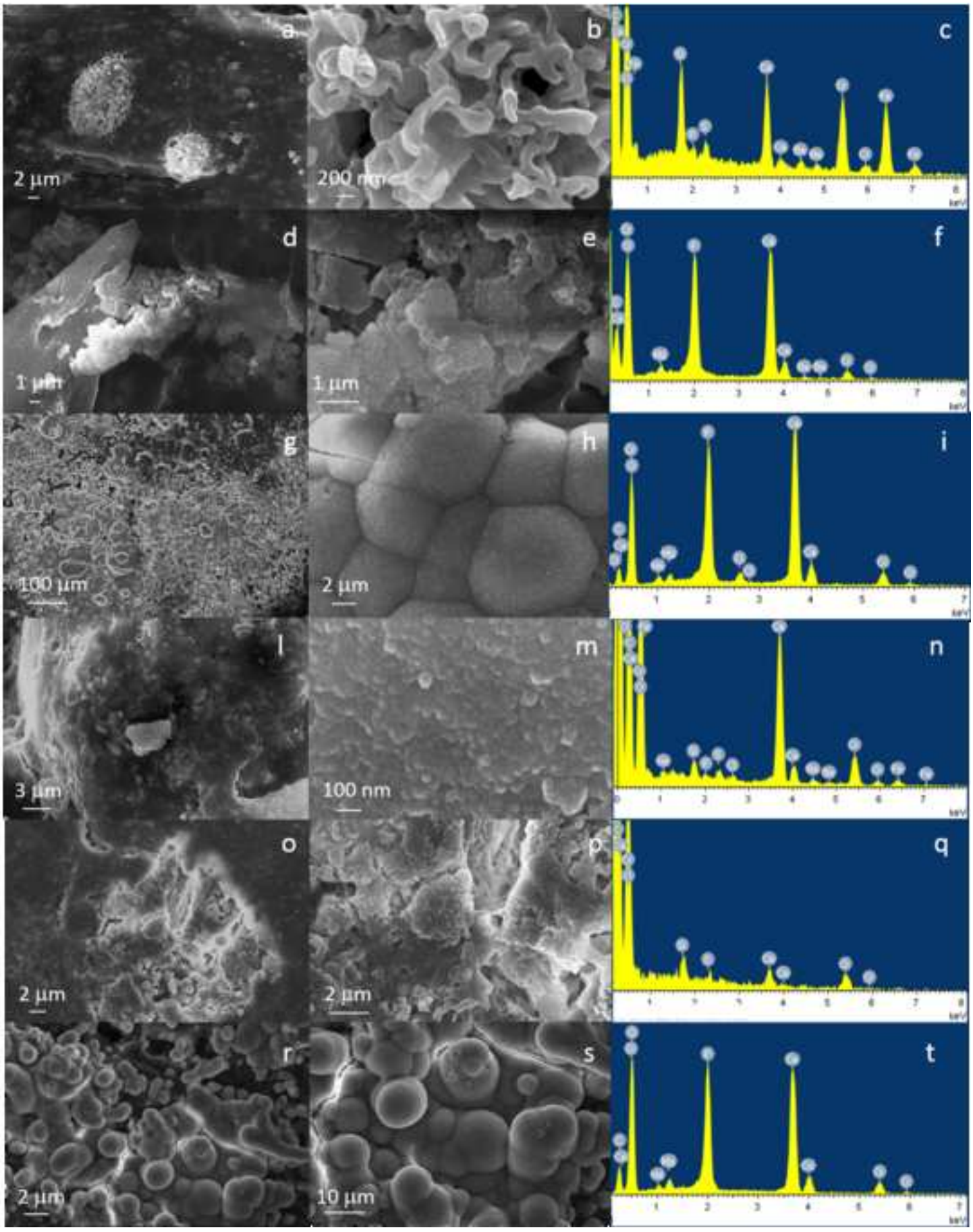

Figure12

Click here to download high resolution image